Journal for Geometry and Graphics
Volume 27 (2023), No. 2, 227–236

Non-Euclidean Descriptive Geometry in Engineering and Applied Visual Arts

Danail Brezov[1], Yana Kancheva[1], Tania Nikova[1,2]

[1] *University of Architecture, Civil Engineering and Geodesy, Sofia, Bulgaria*
danail.brezov@gmail.com, kancheva fgs@uacg.bg

[2] *Bulgarian Academy of Sciences, Sofia, Bulgaria*
tnikova@iomt.bas.bg

Abstract. In this paper we consider the non-Euclidean descriptive geometry of thee-dimensional homogeneous spaces and its possible applications to virtual reality, architecture and design. As a preparation for this mathematical adventure, we first study curved screens in Euclidean space, which are later used in the more general case. Two-dimensional models are used as an illustration of certain features. The geometries of the sphere $\mathbb{S}^3$ and hyperbolic space $\mathbb{H}^3$ are introduced projectively in analogy with the Euclidean case, but with some new peculiar features. Potential applications can be found in optics, relativity and quantum mechanics, visual arts, as well as educational and gaming virtual/augmented reality devices.

Key Words: descriptive geometry, curvature, perspective, virtual reality

MSC 2020: 51N05 (primary), 51M04, 51N15

1 Introduction

Descriptive geometry studies constructively plane projections of three-dimensional bodies (we refer to [6] for a classical introduction) using basic properties of Euclidean, affine and ray spaces as a models for geometric optics (see [2]). It could be thought of as a specific branch of projective geometry, involved more intesively with rulers and compasses than definitions and theorems, which finds plenty of applications in visual arts and engineering graphics. Its linear version in particular involves propagation of light rays in optically flat (with constant refractive index) space and their intersection with a plane, e.g. projection screen, canvas, etc. Both of these restrictions, however, could be violated in a reasonable way which leads to a more general non-Euclidean version of descriptive geometry as well as new potential implementations in the applied branches of science and technology. Partial results in this direction were studied thoroughly a while ago, e.g. the celestial sphere, viewed as a curved projection screen for the night sky, has been in the toolkit of astronomers and sailors for

ISSN 1433-8157/

centuries now. Some authors, however, ignore the fact that the canvas of an artist, drawing objects in hyperbolic space for instance, is flat only with respect to the corresponding metric, but not from Euclidean point of view (see [10]), although curved surfaces are used in all kinds of optical devices and thus, special attention has been paid to them by the physical community (cf. [16]).

The other generalization (allowing non-linear propagation of light) is even more interesting from physical perspective. It appears in classical optics if the media has variable refractive index $n(x, y, z)$, in which case the light trajectories are extremals of the optical path functional

$$\mathcal{S} = \int_{\gamma} n(s)\mathrm{d}s. \tag{1}$$

According to Maupertuis' principle, we may interpret them as geodesics for a suitably chosen metric and the setting is thus equivalent to considering optically flat but geometrically curved space, similarly to the case of gravitational lenses. Such an approach also has the advantage of describing the projective view of an observer inhibiting a non-Euclidean world, which provides straightforward applications in visual tutorials and computer games (see for instance [15]).

Similar considerations apply also to the spherical case, in which the notion of perspective is rather unusual and needs to be dealt with carefully (cf. [13]). More generally, the projection screen (whether flat or not) may be viewed as a two-dimensional section of a system of ODE's

$$\xi \colon \Sigma_0 \xrightarrow{\pi} \Sigma \tag{2}$$

where Σ is the screen surface, while Σ_0 is the set of initial conditions at $t = 0$ representing the visible from Σ part of the object and ξ denotes the vector field generating the flow of light. Its properties determine to a large extend what we would see projected on Σ. For instance, if ξ is Hamiltonian, i.e., $\operatorname{div} \xi = 0$, the phase volume is preserved and one encounters a non-linear analogue of parallel projection in $\mathbb{R}^n$. If, on the other hand, the integral curves of ξ converge, as in $\mathbb{S}^3$, or diverge (as in $\mathbb{H}^3$), we end up with a quite different perspective view of the object.

The geodesic flow $\xi(t)$ on a smooth manifold M is governed by the Jacobi equation (see [2])

$$\ddot{\eta} + \mathcal{R}(\xi, \eta)\xi = 0 \tag{3}$$

where $\mathcal{R}$ stands for the Riemann curvature tensor on M and each solution $\eta \in TM$ of (3), referred to as *Jacobi field*, has the property to deform one geodesic to another. In the case of homogeneous spaces with constant scalar curvature κ, the above equation simplifies greatly for the normal to ξ component, leading to a linear flow in the Euclidean setting, convergent for $\kappa > 0$ and divergent if the curvature is negative. As for the projection map (2), we need it to be single-valued, so ξ has to be regular on Σ_0 and transversal to Σ in order to avoid gliding ray singularities. The screen Σ needs to be a smooth hyper-surface in order to allow infinitesimal analysis, while $\xi(t)$ is continuous on Σ_0 in order to ensure existence of the solutions, and so must be the gradient $\nabla\xi$ if we demand uniqueness as well. Imposing additional restrictions on this rather general setting, we obtain specific examples, such as the spherical and hyperbolic models, considered below. We also discuss visibility, singularities, higher-dimensional extensions and some applications in engineering, design and VR (see [5]).

2 Differential Properties of the Projective Map

As promised, we begin with a 3D model of straight light rays, projected on a smooth curved screen Σ, transversal at all points. Then, the local geometry around a point $p \in \Sigma$ and the

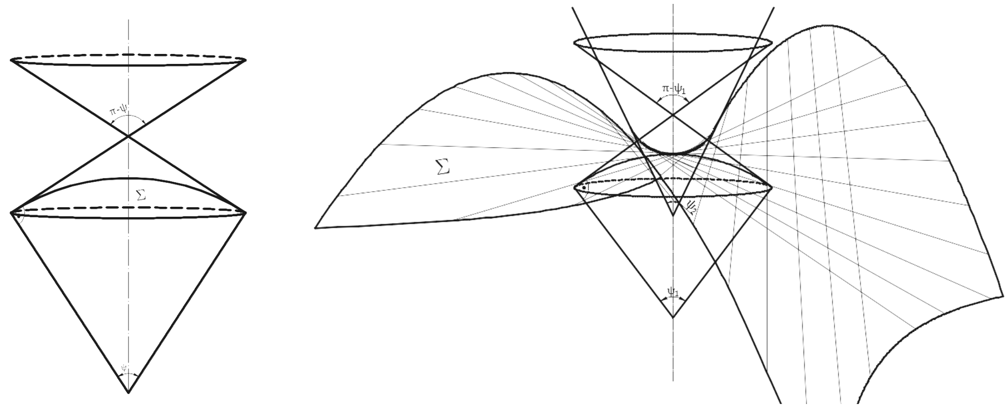

Figure 1: The local cone of view for a convex spherical cap (left) and a saddle point on a hyperbolic ruled surface (right).

angle by which the light rays through p hit Σ together determine the properties of the image at p, such as visibility and distortion. We shall discuss both parallel and central projections, while orthogonal projection is not typical in this setting and it may occur only under very specific conditions, as explained below. However, we should go back to it once we allow light to travel along curved trajectories - a case that is only briefly commented on in this section.

2.1 Image Distortion

Let us consider for now a Hamiltonian (hence, incompressible) flow (2). The image on Σ will then be a distorted version of the one carried by ξ due to both the variable angle, at which the light rays hit the surface and the non-trivial metric[1] on Σ, given as $\mathrm{d}s^2 = g_{ij}(x)\,\mathrm{d}x^i\,\mathrm{d}x^j$. If we allow the vector field ξ in (2) to have a non-zero divergence, then apart from distorsion, we may end up also with caustics and change of orientation, as any child who has played with optical lenses may confirm. In the examples of homogeneous geometries below, we shall encounter this effect and discuss its relation to equation (3), but for now let us focus on the above two properties. The former one is a well known effect of non-orthogonal projection causing problems for example in construction of optical devices (see [7]). In short, the infinitesimal area is stretched (and the intensity - diminished) by a factor, reciprocal to the sine of the angle, at which the light rays hit the surface. The second effect, on the other hand, is entirely due to the geometry of the projection surface, which is encoded in the metric and its derivatives. In particular, if the metric of Σ is conformally flat, one may simply use the corresponding conformal factor as a measure of curvature-related image distortion. For instance, instead of working with the usual metric on $\mathbb{S}^2$ given in terms of the azimuth ϑ and the polar angle φ:

$$\mathrm{d}s^2 = \mathrm{d}\vartheta^2 + \sin^2\vartheta\ \mathrm{d}\varphi^2 \tag{4}$$

one may cnange the representation, and use the projective Fubini-Study metric, expressed as

$$\mathrm{d}s^2 = \frac{|\,\mathrm{d}z|^2}{(1+|z|^2)^2}, \quad z \in \mathbb{CP}^1 \cong \mathbb{C} \cup \infty. \tag{5}$$

To study the (curvature-based) deformation in the principal directions at each point of Σ one may use the ratio $\lambda \in [0,1]$ between the areas of the flat and curved projections (Figure 1).

[1]Here and below we shall assume summation over repeated indices.

For a spherical cap with solid angle 2ψ with $\psi \in [0, \pi]$, the coefficient of distortion is equal to

$$\lambda = \cos^2 \frac{\psi}{4}. \tag{6}$$

In general, the two principle curvatures may differ (see [12]), thus giving rise to a pair of angles $\psi_{1,2}$ associated with the two osculating circles of radii $R_{1,2}$. Then, one encounters elliptical or hyperbolic region, depending on the sign of the sectional curvature, while it vanishes in the limit $R_1 \to \infty$ ($\psi_1 = \pi$) that yields for cylindrical surfaces the ratio $\lambda = \frac{2}{\psi} \sin \frac{\psi}{2}$. An exact formula for λ may be derived for a generic quadric, but on the infinitesimal level this coefficient is point-wise related to the inverse Jaccobian for the smooth projection surface[2] Σ

$$J^{-1} = \det\left(\frac{\partial y^i}{\partial x^j}\right). \tag{7}$$

2.2 Visibility

Let us now assume that Σ is a spherical cap of radius R and solid angle 2ψ sliced from the sphere by a central cone with angle at the vertex equal to ψ (Figure 1). It is clear that the curved surface of the screen may cast shadow if the angle, at which the light hits, is small enough. Basic geometry shows that the directions of parallel light rays that illuminate the entire screen are contained in the interior of a coaxial (with the line of symmetry) cone, whose angle ϑ at the vertex and distance from it to the centre of the sphere are given explicitly as

$$\vartheta = \pi - \psi, \quad d = R \sec \frac{\psi}{2}. \tag{8}$$

In particular, if the screen is a hemisphere $\psi = \pi$, the only direction with such property is obviously the axis of rotational symmetry $\vartheta = 0$, i.e., $d = \infty$. Note that this holds no matter if the screen is convex or concave from the perspective of the light source as the two cones are dual in a way, namely as the one with vertex at the centre of the sphere becomes a boundary of visibility in the concave case, while the other plays the role of a projection screen. Similar arguments are applicable in the case of perspective projection when infinite points are involved. In this setting, however, we deal not with the double cone, but only with one of its branches: in the convex case this is the more distant one, while if the screen is concave viewed from the object, we only consider the part of the cone that lies in front of it (Figure 1).

Now, let us abandon the assumption of axial symmetry, allowing the screen surface to have different principal curvatures. The region of visibility would generally be an elliptical cone with semi-axes given by the radii of the cones corresponding to the two osculating circles at each parallel slice (see Figure 1). This holds both for positive and negative sectional curvature, while for $K = 0$, e.g. at a fold-type singularity, one of the semi-axes becomes infinite and the ellipse degenerates to a pair of parallel lines. Finally, applying this idea locally, in a vicinity of each separate interior point of Σ, we obtain the field of view as intersection of a continuous family of cones: both in the parallel and perspective projection setting. Typically, however, one deals with algebraic surfaces: the loci of quadrics, or possibly cubics, which are not that rippled and exact closed form analytical treatment is still available, although not quite trivial.

[2] Here the y^i's denote the local coordinates on Σ.

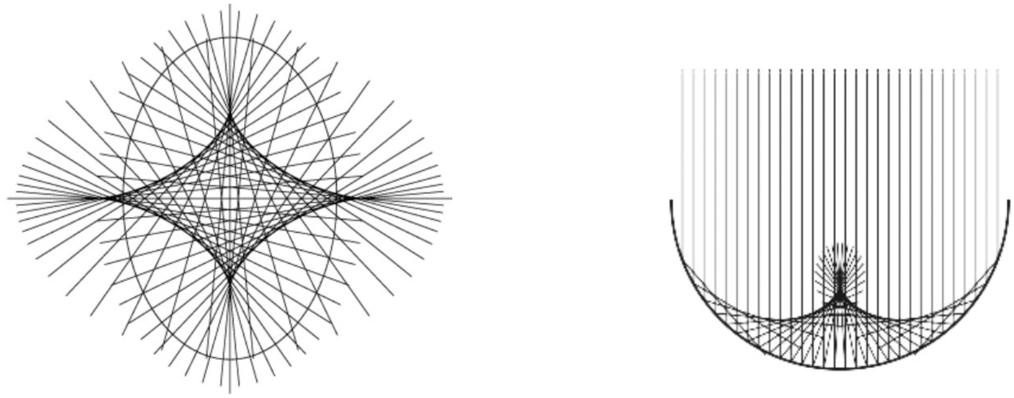

Figure 2: Two examples of caustics: the evolute of an ellipse as an envelope of the set of normal rays (left) and one often used for amplification of signals in parabolic satellite dishes (right).

2.3 Singularities

In our previous considerations we always assumed that the light rays, whether straight or curved, are transversal to the screen surface at all points and the reason to do that was to avoid the so-called *gliding ray singularity*, in which the image of a point form the object's visible area Σ_0 is a degenerate one-parameter set, i.e., the map (2) is not a projection anymore. This effect is well known from the moon path formed on a calm water surface and has been used in optical cables to transmit high frequency signals. A gliding singularity on the surface Σ means that points in the object Σ_0 end up being mapped into line segments on the screen.

There are other more complex types of singularities that are also relevant to actual problems in physics and engineering. One example familiar from geometric optics are the so called *caustics* (see [4, 14]), usually studied in the context of catastrophe theory[3]. Caustics, which explain various optical effects, such as the rainbow or the purges against ants executed with a magnifying glass, are defined in geometric terms as *envelopes* of families of light rays, i.e., curves or surfaces, to which there is a light ray tangent at each point. If a projection screen happens to intersect a caustic of the light field, the so obtained image may be quite unusual.

The overlap of images under the projection map (2) in the presence of caustics is an obstruction to retrieving the geometric information about the pre-image Σ_0 it encodes, as violates the injectivity. Similarly, gliding rays make (2) multi-valued, in which case the inverse is not injective either. This effect may be observed even in Euclidean projections if we choose the screen Σ in the form of a *ruled surface* and let one of the light rays coincide with a generator[4].

There are certainly other problems that may interfere with the back-tracing of image points to the object, apart from singularities. For example, the flow generated by $\xi(t)$ could be mixing or even chaotic, in which case all information is lost and we can do nothing but enjoy the view. To eliminate these problems one may impose restrictions on both ξ and the surfaces in (2) to guarantee regularity, i.e., existence and uniqueness of the integral curves, hence invertibility.

[3]For a systematic and yet comprehensive study of catastrophes, with emphasis on the applications, see [9].

[4]Combined with a good use of optics, these geometries provide interesting opportunities for visual effects.

3 Intrinsic Geometry of Homogeneous Spaces

So far we speculated over a possible straightforward generalization of Euclidean descriptive geometry, in which the projection planes are replaced with smooth surfaces and light propagates along the integral curves of a system of ODE's. In particular, parallel rays are solutions corresponding to different initial conditions of the Cauchy problem, assuming it is well posed. As mentioned above, an alternative way to look at this situation is attributing the optical properties of the medium to some intrinsic geometry (metric structure, connection form and curvature). As we know from both Newtonian mechanics and relativity, the paths along which light propagates are extremals of some action functional and may be interpreted as geodesics.

3.1 Euclidean Geometry via Projection

It is often pointed out that classical Euclidean planimetry may be studied projectively, as an image of events that occur in three-dimensional space, mapping rays though the origin in $\mathbb{R}^3$ to points in the projective plane $\mathbb{RP}^2$ respectively, planes through the origin to lines and pencils of rays - to curves. Going up a dimension, we may consider problems of stereometry, and descriptive geometry in particular, similarly introducing homogeneous coordinates in $\mathbb{R}^4$

$$\mathbf{X} \in \mathbb{R}^4 \mapsto x^i = \frac{X^i}{X^0}, \quad i = 1, 2, 3 \tag{9}$$

which yield with the above constriction projective coordinates in $\mathbb{RP}^3$. Thus we have a central projection from the origin in $\mathbb{R}^4$ to the plane $X^0 = 1$. A plane $\alpha \subset \mathbb{RP}^3$ is lifted to a hyperplane

$$\alpha\colon a_0 + a_i x^i = 0 \mapsto \tilde{\alpha}\colon a_\mu X^\mu = 0, \quad \mu = 0, 1, 2, 3 \tag{10}$$

through the origin $\tilde{\alpha} \subset \mathbb{R}^4$ according to (9), and we may use the same construction for points, lines, quadrics and all sorts of geometric objects with analytic description in $\mathbb{R}^3$, which is now regarded as an open patch of the compact $\mathbb{RP}^3$. Note, however, that one-dimensional subspaces (lines through the origin) in $\mathbb{R}^4$ are also described by their traces on the unit three-sphere $\mathbb{S}^3$, which is another possible "hyper-screen" to depict four-dimensional events. Thus, we have a natural correspondence between the two descriptions $\mathbb{S}^3 \to \mathbb{RP}^3$ that identifies antipodal points and is given explicitly also by (9), this time with the additional restriction

$$X_\mu X^\mu = 1 \tag{11}$$

on the homogeneous coordinates. The two-dimensional model provides some intuition for this relation. For instance, it shows that great circles (the geodesics on the sphere) are mapped to straight lines (the geodesics in the plane) and in particular, meridians — to lines through the origin, while the equator plays the role of *line at infinity*. Thus, two big circles intersecting on the equator of $\mathbb{S}^2$ are viewed as parallel lines in the plane projection and similarly, conic sections are classified with respect to the number of intersection points with the equator of the corresponding pre-image (generic circle) on $\mathbb{S}^2$. Using another type of projection, however, e.g. stereographic, we see quite a different picture in the plane: circles on $\mathbb{S}^2$ incident with the south pole are now mapped to straight lines and those with no other common point appear parallel (meet at infinity). Note that stereographic projection does not identify antipodal points on the sphere and may thus be seen as a compactification of the Euclidean plane (with just one point at infinity instead of a whole line), rather than projectivization. However, it is a good way to depict spherical geometry in the plane and has lots of applications [7].

3.2 Spherical and Hyperbolic Geometry

The spherical version of 3D projective geometry is quite similar to the above construction: with 2-spheres embedded in $\mathbb{S}^3$ corresponding to either planes though the origin or quadrics in $\mathbb{RR}^3$, the equator now playing the important role of a plane at infinity. The angle is preserved under projection only if the corresponding intersection in $\mathbb{S}^3$ is incident with the north pole, i.e., the origin in the flat picture. This allows us to generalize the Monge apparatus from the Euclidean case to mutually perpendicular spherical screens. Central projection, however, is associated with perspective view, and in the spherical setting the point of view plays a crucial role for the final result. A classical example is given by the famous stereographic projection

$$\tilde{x}^i = \frac{2X^i}{1+X^0} = \frac{2x^i}{1+\sqrt{1+\mathbf{x}^2}}, \qquad X_\mu X^\mu = 1 \tag{12}$$

where the x^i's denote the coordinates of the (perspective) projection and $\{\tilde{x}^j\}$ are the ones corresponding to the stereographic projection. Note that one may choose to project on a generic horizontal hyper-plane $X^0 = \lambda \geq 0$, in which case one needs to substitute the factor 2 with $\lambda + 1$ and the above formula still works. This way we obtain different versions of the famous "fish eye" perspective. It is also straightforward to derive the inverse transformation

$$X^i = \frac{2\tilde{x}^i}{1+\tilde{\mathbf{x}}^2}, \quad X^0 = \frac{1-\tilde{\mathbf{x}}^2}{1+\tilde{\mathbf{x}}^2}. \tag{13}$$

In order to study the descriptive geometry of hyperbolic space in a similar way, we assume that there is a 4D correspondence space between the flat and hyperbolic projection. It needs to have non-trivial signature so that it is compatible with the negative curvature of the quotient (upper half-space or unit ball model) and still projects nicely onto $\mathbb{R}^3$. Thus, we end up with

$$X_\mu X^\mu = X_0^2 - X_1^2 - X_2^2 - X_3^2 \tag{14}$$

which may be positive, negative or vanishing depending on the direction chosen, and defines $\mathbb{R}^{1,3}$, the flat pseudo-Euclidean space with scalar square. In particular, directions with vanishing scalar square are called *isotropic* and form a three-dimensional cone (referred to as *light cone* in physics), serving as a boundary between the hyperbolic and elliptic regions. Now, consider $\mathbb{R}^3$ as a horizontal slice of $\mathbb{R}^{1,3}$, e.g. with the hyperplane $X^0 = 1$, which we may use as canvas for central projection and thus, interpret Euclidean stereometry projectively also in pseudo-Euclidean context. In particular, the isotropic cone is mapped to the unit sphere in $\mathbb{R}^3$ and the hyperplane $X^0 = 0$ again becomes the plane at infinity. Another non-Euclidean canvas for projection here would be the unit hyperboloid given in homogeneous coordinates as $X_\mu X^\mu = 1$. It yields a natural relation between the flat and hyperbolic projective pictures and an analogue of (12) and its inverse (13) in the form (assuming that $X_\mu X^\mu = 1$ and $X^0 \geq 0$)

$$\tilde{x}^i = \frac{2X^i}{1+X^0} = \frac{2x^i}{1+\sqrt{1-\mathbf{x}^2}}, \qquad X^i = \frac{2\tilde{x}^i}{1-\tilde{\mathbf{x}}^2}, \quad X^0 = \frac{1+\tilde{\mathbf{x}}^2}{1-\tilde{\mathbf{x}}^2}. \tag{15}$$

Note also that choosing another projection hyperplane in $\mathbb{R}^{1,3}$ one generally obtains quite a different picture, but the metric in the projection would always be nontrivial, with an isotropic cone, elliptic and hyperbolic regions. Moreover, unlike the sphere, $\mathbb{H}^3$ is open — similarly to Euclidean space, but it has other peculiar features, such as divergent geodesic flow (see [1]).

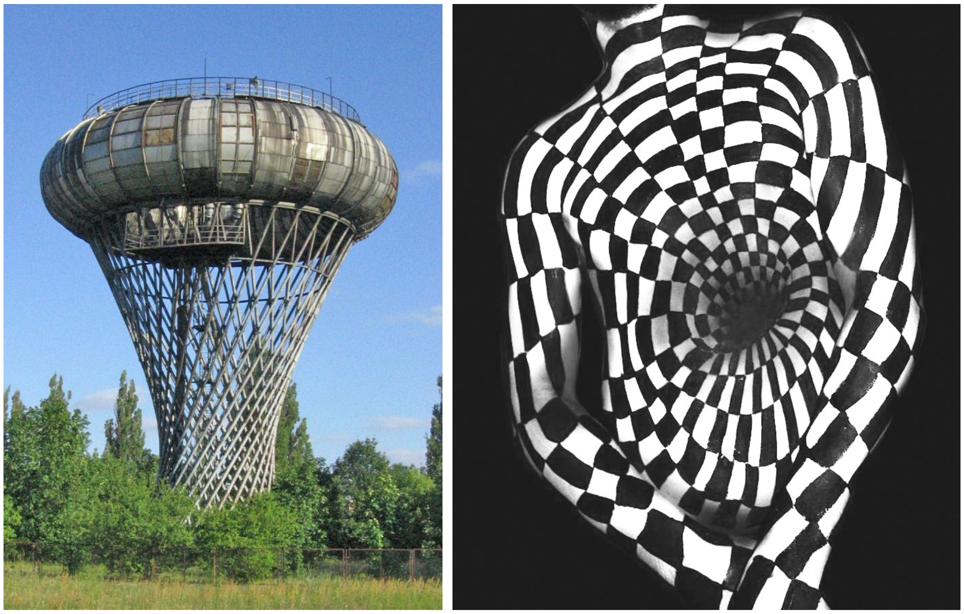

Figure 3: Ruled hyperbolic water tower (left; created by Wikipedia user Kaczorgw under license CC BY-SA 3.0) and optical illusion in body painting (courtesy of Natalie Fletcher).

4 Geometric Properties and Applications

Probably the most exotic features of spherical descriptive geometry come from the fact that unlike the Euclidean plane, $\mathbb{S}^3$ is compact, so it contains all its limits. In particular, one can reach the horizon (the equatorial "plane" in $\mathbb{S}^3$) in no time with the proper means of transportation, even cross it, thus undergoing a full reflection. In this sense, it has a function of a natural geometrical lens: an object that is halfway through would look skew from each hemisphere and seen from the horizon all object appear as points. Moreover, smart travelers (including photons) move along great circles, which plays the role of straight lines. Similarly, 2-spheres substitute flat planes and one may choose three mutually perpendicular ones (meridians) through the north pole as coordinate planes. Close enough to this point (mapped to the origin in $\mathbb{R}^3$), things look pretty "straight", but as we go farther, some unusual effects appear. For instance, the orientation of vectors generally changes under parallel transport due to the curvature of $\mathbb{S}^3$, which is visible in two dimensions as well. On the other hand, 360° view is now available without any fisheye technology involved, e.g. an object on the south pole can be "seen" in clear weather from the north pole simultaneously from all angles.

Similarly, in hyperbolic space geodesics violate Euclid's fifth principle, allowing for infinitely many parallels to a given line to be build through a given point. This makes some constructions of descriptive geometry rather unusual. Certainly, there is a flat realization with non-definite metric (Minkowski space) but in that case one has an isotropic cone, on which directions can be both parallel and orthogonal. All these effects may be attributed to various types of singularities, as we already discussed above. To avoid such complications it is convenient to consider Monge projections for example simply as intersections. One particular illustration of this non-euclidean Monge geometry can be seen in the phase portrait of a dynamic system (Figure 4). The space-time and phase-space sections provide the usual graphic expressions, the dynamic flow plays the role of light and the observable is just the initial data.

Non-Euclidean geometry has found plenty of application in architecture and design of all ages: the impressive medieval cathedrals confirm this together with modern hyperbolic

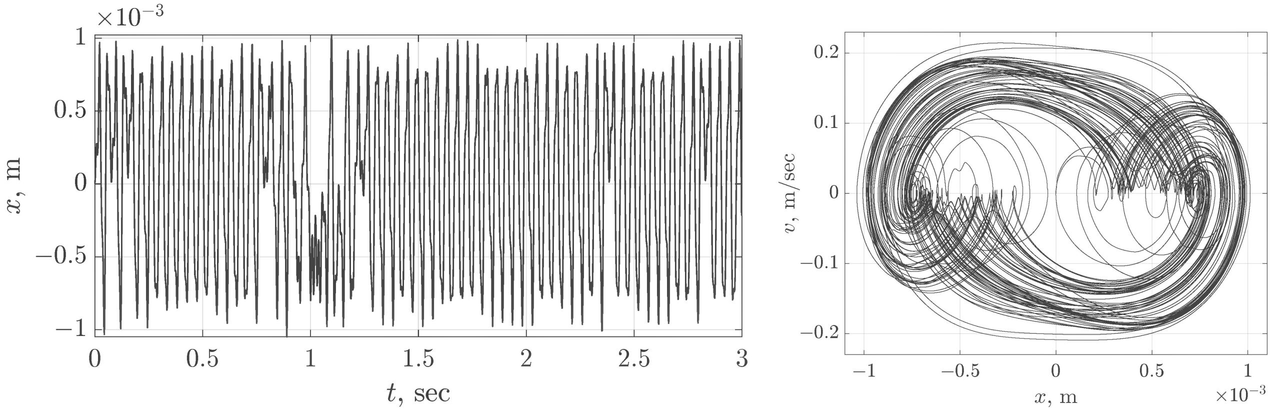

Figure 4: Phase portrait and time-motion of the Duffing oscillator as a Monge projection.

constructions, such as roofs or lattice towers [3, 8] and the famous works of Gaudi [11]. The appreciation for hyperbolic shapes in modern constructions dates back to the end of the 19th century when Vladimir Shukhov presents two pavilions with doubly curved gridshells at the All-Russian Industrial and Handicrafts Exposition in 1896. Shikhov continues working on optimizing the design using the mathematical background of approximation of functions for the purpose of minimizing labour, materials and time in construction. Around the same period, Antoni Gaudi includes elements of hyperbolic geometry in the design of Sagrada Familia and Park Güell in Barcelona. Currently non-Euclidean shapes are symbol of advanced and creative architecture and the dimensions have been scaling up over the past few decades. The result is an ongoing precision of architectural design, variety of thin-shelled structural shapes popularized by many architects, e.g. Zaha Hadid, Santiago Calatrava, Oscar Niemeyer and many others. Non-Euclidean design is used for industrial (cooling or water towers, factories), office and residential buildings, hotels, monuments, amusement parks, transportation facilities (stations, bridges, tunnels), urban planning etc. Curved spatial elements can be found in both western and eastern architecture ever since we have had the mathematical knowledge and industrial technology to implement them. The reason for such success is partly practical, e.g. constructional stability (vaults, domes, bridges, helical stairs), optimized aero and thermodynamics (aircraft and spacecraft vehicles, cooling towers), acoustic and optical properties (musical instruments, concert halls, telescopes, satellite dishes), or just simplicity, as in the case of ruled surfaces. There is, on the other hand, a purely esthetic motivation for including concepts of spherical and hyperbolic geometry in architecture and design: from the stained glass art in orthodox churches and catholic cathedrals, to ancient Indian mandalas and their modern versions involving tessellations of the Poincaré disc model of the hyperbolic plane that once captured the attention of M. C. Escher, who turned it into a hit. There is hardly need to motivate our interest in the subject any further, let us just point out a relatively new context, in which non-Euclidean descriptive geometry appears quite naturally, namely, the art of optical illusion [5]. Some artists use flat canvas (e.g. streets and buildings), to create a three-dimensional sensation when the painting is seen from a certain angle, others prefer curved surfaces, such as the human body (Figure 3). Modern technologies, such as holography and virtual reality, provide an opportunity for visual arts to reach new frontiers.

Acknowledgments: This publication has been funded by the University of Architecture, Civil Engineering and Geodesy.

References

[1] L. Ahlfors: *Möbius Transformations in Several Dimensions*. University of Minnesota, 1981.

[2] V. Arnold: *Mathematical Methods of Classical Mechanics*. Springer, New York, 1978.

[3] M. Beckh: *Hyperbolic Structures: Shukhov's Lattice Towers - Forerunners of Modern Lightweight Construction*. Wiley-Blackwell, 2015.

[4] M. Berry and C. Upstill: *Catastrophe Optics: Morphologies of Caustics and Their Diffraction Patterns*. Progress in Optics **18**, 257–346, 1980. ISSN 0079-6638.

[5] R. Carraher and J. Thurston: *Optical Illusions and the Visual Arts*. Reinhold Pub. Corp., Michigan, 1966.

[6] C. Davies: *Elements of Descriptive Geometry with Their Applications to Spherical Trigonometry, Spherical Projections and Warped Surfaces*. A. S. Barnes & Co., New York, 1866.

[7] M. Fleck: *Perspective Projection: The Wrong Image Model*. Tech. rep., Department of Computer Science, University of Iowa, 1970.

[8] E. Gawell: *Non-Euclidean Geometry in the Modelling of Contemporary Architectural Forms*. The Journal of Polish Society for Geometry and Engineering Graphics **25**, 35–43, 2013.

[9] R. Gilmore: *Catastrophe Theory for Scientists and Engineers*. John Wiley & Sons, New York, 1981.

[10] V. Hart, A. Hawksley, E. Matsumoto, and H. Segerman: *Non-Euclidean Virtual Reality I: Explorations of H3*, 2017. arXiv: `1702.04004`.

[11] S. Huerta: *Structural Design in the Work of Gaudí*. Architectural Science Review **49**(4), 324–339, 2006. doi: `10.3763/asre.2006.4943`.

[12] B. O'Neill: *Elementary Differential Geometry*. Elsevier, London, 1966.

[13] C. Soddu: *Perspective, a Visionary Process: The Main Generative Road for Crossing Dimensions*. In T. García-Salgado, ed., *Architecture, Mathematics and Perspective*, 33–46. Birkhäuser, Basel, 2010. doi: `10.1007/978-3-0346-0518-2_3`.

[14] O. Stavrodis: *The Optics of Rays, Wavefronts and Caustic*. Academic Press, London, 1972.

[15] J. Weeks: *Curved Spaces, a flight simulator for multiconnected universes*. `http://www.geometrygames.org/CurvedSpaces/`.

[16] M. Šarbort: *Non-Euclidean Geometry in Optics*. Ph.D. thesis, Masaryk University, Brno, 2013.

Received April 21, 2023; final form July 31, 2023.